Epidemics 8 (2014) 18–27

Contents lists available at ScienceDirect

Epidemics

journal homepage: www.elsevier.com/locate/epidemics

The influence of changing host immunity on 1918–19 pandemic dynamics

K.J. Bolton[a,b,*], J.M. McCaw[b,c], J. McVernon[b,c], J.D. Mathews[b]

[a] School of Mathematical Sciences and School of Community Health Sciences, University of Nottingham, University Park, NG7 2RD, United Kingdom
[b] Centre for Epidemiology and Biostatistics, Melbourne School of Population and Global Health, University of Melbourne, 3010, Australia
[c] Murdoch Childrens Research Institute, Royal Childrens Hospital, 3052, Australia

ARTICLE INFO

Article history:
Received 27 November 2013
Received in revised form 1 July 2014
Accepted 30 July 2014
Available online 8 August 2014

Keywords:
Influenza
Transmission models
Immunology
Viral evolution
Public health

ABSTRACT

The sociological and biological factors which gave rise to the three pandemic waves of Spanish influenza in England during 1918–19 are still poorly understood. Symptom reporting data available for a limited set of locations in England indicates that reinfection in multiple waves occurred, suggesting a role for loss of infection-acquired immunity. Here we explore the role that changes in host immunity, driven by a combination of within-host factors and viral evolution, may play in explaining weekly mortality data and wave-by-wave symptomatic attack-rates available for a subset of English cities. Our results indicate that changes in the phenotype of the pandemic virus are likely required to explain the closely spaced waves of infection, but distinguishing between the detailed contributions of viral evolution and changing adaptive immune responses to transmission rates is difficult given the dearth of sero-epidemiological and virological data available even for more contemporary pandemics. We find that a dynamical model in which pre-pandemic protection in older "influenza-experienced" cohorts is lost rapidly prior to the second wave provides the best fit to the mortality and symptom reporting data. Best fitting parameter estimates for such a model indicate that post-infection protection lasted of order months, while other statistical analyses indicate that population-age was inversely correlated with overall mortality during the herald wave. Our results suggest that severe secondary waves of pandemic influenza may be triggered by viral escape from pre-pandemic immunity, and thus that understanding the role of heterosubtypic or cross-protective immune responses to pandemic influenza may be key to controlling the severity of future influenza pandemics.

Introduction

The "Spanish" influenza pandemic of 1918–19 was responsible for tens of millions of deaths worldwide. Despite pre-dating the isolation of the influenza virus, epidemiological records from the 1918 influenza pandemic have allowed much to be inferred about the transmission characteristics of the 1918 pandemic virus (henceforth pH1N11918) (e.g. Fraser et al., 2011; Valleron et al., 2010). However the ecological conditions which gave rise to the three distinct peaks of mortality over a period of just nine months in England and Wales (Smallman-Raynor et al., 2002; Pearce et al., 2011) remain intriguing.

Virological and genealogical studies of the 1918 pandemic virus, whilst based on limited genetic samples, imply that pH1N11918 had been circulating in mammals for several years prior to the pandemic, and likely co-circulated with seasonal and swine lineages of H1N1 (Smith et al., 2009; dos Reis et al., 2011). In more contemporary pandemics severe second waves of pandemic transmission may have been triggered by changes in the circulating virus (Viboud et al., 2005). Heterosubtypic immunity mediated by cellular responses or cross-reactive antibody is relevant even for novel pandemic influenza viruses (Grebe et al., 2008), and probably influenced cohort disease severity in more recent pandemics (Slepushkin, 1959; Epstein, 2006). Multi-wave epidemics such as that observed in England in 1918–19 offer rare opportunities to infer the nature of short-term shifts in adaptive protection and/or viral evolution.

Circulation of multiple viral phenotypes, loss of adaptive immunity, and variable transmissibility have been considered as mechanisms in models for pandemic influenza transmission and mortality in 1918–19 (Shi et al., 2010; He et al., 2011; Mathews

* Corresponding author at: School of Mathematical Sciences and School of Community Health Sciences, University of Nottingham, University Park, NG7 2RD, United Kingdom. Tel.: +44 7774582526.
E-mail addresses: kirsty.bolton@nottingham.ac.uk (K.J. Bolton), jamesm@unimelb.edu.au (J.M. McCaw).

http://dx.doi.org/10.1016/j.epidem.2014.07.004

Table 1
Patterns of symptom reporting per thousand head of population for 5 cities. Entries under each heading N_{ijk}, $i, j, k \in \{0, 1\}$ correspond to the number of people (per unit thousand) who reported illness in waves 1, 2 and/or 3 if i, j and/or $k = 1$, respectively. The second to last column shows the total surveyed population (N_{survey}) and the final column the total population size (N). The final row shows the symptom reporting pattern for the composite data set.

City	N_{111}	N_{101}	N_{011}	N_{001}	N_{110}	N_{100}	N_{010}	N_{survey}	N_{total}
Blackburn	0.778	4.67	7.78	64.6	5.45	75.5	56.1	1284	113 000
Leicester	0.432	4.76	8.01	69.9	3.03	62.1	135	4619	213 000
Manchester	0.640	5.54	2.34	15.6	14.3	131	83.6	4686	659 000
Newcastle	0.448	8.74	3.81	73.0	0.448	52.4	46.6	4461	267 000
Wigan	0.930	0	1.86	108	0	40.9	73.4	1075	83 000
Composite	0.558	5.76	4.77	57.1	5.58	79.0	85.3	16 125	1 335 000

et al., 2007, 2010). In some regions changes in population mixing due to mandatory or reactive social distancing may be sufficient to explain second peaks of disease (Bootsma and Ferguson, 2007; Caley et al., 2008). It is not clear that social distancing was widespread in the UK in 1918–19 (Ministry of Health, 1920), however recently He et al. employed a stochastic transmission model to demonstrate that reactive social distancing, supplemented by seasonal and school-term effects, was a plausible mechanism for generating the variation in transmission rates required to reproduce the pattern of mortality in England and Wales (He et al., 2013). Dynamical models in which transmissibility is modulated only by social mixing effects cannot explain records of multiple symptomatic infections over the course of the 1918–19 pandemic (Ministry of Health, 1920). In previous work, motivated by epidemiological evidence indicating recent exposure to influenza can provide some lasting heterologous protection against symptomatic disease (Slepushkin, 1959; Barry et al., 2008), viral shedding (McMichael et al., 1983) and/or laboratory confirmed influenza (Wilkinson et al., 2012; Epstein, 2006), we have shown that loss of pre-pandemic and acquired adaptive protection likely played a significant role in the transmission dynamics of the 1918 pandemic (Mathews et al., 2007, 2010). In this paper we present a set of dynamical models for pandemic influenza transmission with various immunologically motivated prescriptions for the behaviour of pre-pandemic and adaptive immunity that do not *a priori* assume the emergence of new viral phenotypes over the course of the pandemic. We compare the ability of candidate models to fit composite mortality and symptom reporting data from 1918 to 1919 for a set of English cities. We discuss the plausibility and interpretation of these models and the consequences of our findings for predicting the severity of future pandemic outbreaks.

Methods

Data and historical context

The influenza pandemic of 1918–19 killed approximately 2 per cent of the population in the United Kingdom with excess mortality in England estimated to be ~0.3% (Murray et al., 2006). The herald summer wave was characterised by very high morbidity and a marked shift towards mortality in younger age groups (e.g. Nguyen-Van-Tam and Hampson, 2003). The following autumn wave was the most severe; with the highest death rates and case fatality ratios. Records of the succeeding winter wave characteristically note a decrease in death count relative to the autumn wave (see Chowell et al., 2008, and references therein).

There is inconclusive evidence of changes in the virus during 1918–19. Genetic analyses of the partial viral isolates recovered suggest that at least two lineages of H1N1 were in circulation (Reid et al., 2003, 2004; Taubenberger and Morens, 2006; Morens and Fauci, 2007). Clinical notes indicate changes in disease severity over the course of the pandemic: an incongruence between the mild symptoms of the summer wave and the severe autumn wave was mentioned, and doctors speculated that the pathogen circulating in the winter may have been different again (Ministry of Health, 1920, p. 144). Mean hospitalisation rates in US army training camps were also lower in the first than subsequent wave (Barry et al., 2008).

Table 2
Summary of prior and acquired immunity characteristics of candidate models.

Acquired	Prior			
	None	Sustained	Temporary	
			Constant	Variable
Constant	A1	B1	C1	D1
Boosted	A2	B2	C2	D2

The Medical Officer for Health in Manchester describes recommendations that citizens were advised to avoid large social gatherings and attend to personal hygiene in order to minimise their risk of contracting influenza (Ministry of Health, 1920, p. 471). There are also reports of school closures in Manchester during the summer wave. However, cinemas, churches and theatres were reported to have operated largely unhindered with small changes in regulations such as improved ventilation, cancelled Sunday school classes, and the prohibition of pre-teenage children into cinemas/theatres. We are unaware of the degree of recommended and reactive social distancing in the other cities under study here and do not take into account any social distancing effects in our model.

We have aggregated weekly mortality data for the period 29th June 1918–10th May 1919 and wave-by-wave symptom reporting data for five English cities (Blackburn, Leicester, Manchester, Newcastle and Wigan) as reported by the Ministry of Health (Ministry of Health, 1920) into a "composite" data set *representative* of the epidemic in mid-north England. Note that we do not assume that the composite data set is generated by homogeneous mixing between the 5 cities from which the data was collected. Error bars for composite data points are calculated using bootstrapping methods (Efron, 1979). Our aggregation will average over spatial heterogeneities, which reflect the spatial diffusion of the pathogen (Smallman-Raynor et al., 2002; Eggo et al., 2010). However the cities that have symptom reporting data available are all located in mid-north England and have epidemics of similar timing.[1] Symptom reporting data is reproduced in Table 1, and the composite mortality data is shown in Fig. 2. We append 15 null weekly death counts to the mortality data in order to penalise models that predict unobserved waves of infection when performing model fitting.

Model structure

We trial eight candidate models, grouped into families A–D, as summarised in Table 2. All candidates are simple modifications

[1] The autumn wave in the most southerly city Leicester is slightly delayed compared to the other cities.

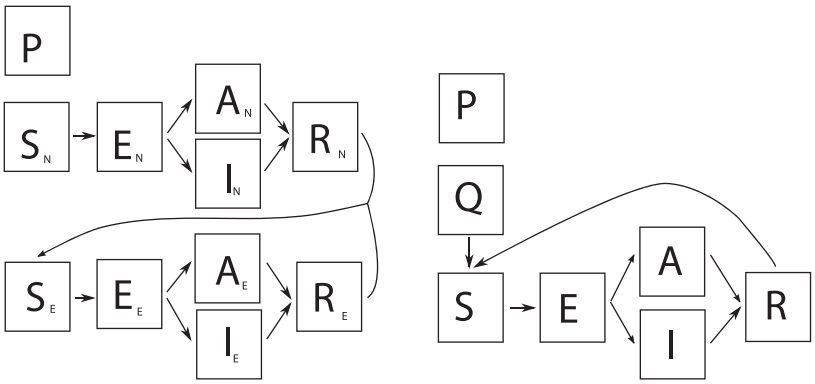

(a) Model families A & B: Sustained partial prior immunity (b) Model families C & D: Waning sterilising prior immunity

Fig. 1. Basic compartmental model configuration for models with (a) absent or sustained partial prior immunity or (b) waning/temporary sterilising prior immunity. In (a) the subscripts 'E' and 'N' refer to influenza-experienced and naïve hosts respectively, with the former exhibiting lower susceptibility, infectiousness and propensity to report symptoms. In (b) the compartment Q represents hosts who are initially protected. Susceptible hosts become exposed at a rate $\beta \propto R_{\text{eff}}(t)$. Waiting times between other compartments are described by an Erlang-2 distribution with rate parameter ϕ_{wQ} ($Q \rightarrow S$), ϕ_w ($R \rightarrow S$), $1/T_e$ ($E \rightarrow I$) or $1/T_i$ ($I \rightarrow R$). All candidate models also allow for a proportion x_I of hosts with sustained sterilising pre-pandemic immunity, captured by an isolated compartment P as described in the main text.

of an **S** (Susceptible)–**E** (Exposed)–**I** (Infectious)–**A** (Asymptomatically infectious)–**R** (Recovered) model for pandemic influenza virus transmission, as shown in Fig. 1 and in greater detail in Supplementary Material Figures S1–S4. Common to all models is the assumption that the basic reproduction number changes only due to a seasonal forcing term, but the symptomatic reporting proportions α_i and case fatality rates μ_i are independent for each wave ($i \in \{1, 2, 3\}$). Asymptomatic infections may correspond to sub-clinical infections or unreported disease. Deterministic epidemic dynamics become unrealistic when the number of infections becomes very small, as may occur during inter-wave periods. To ensure each wave is initiated at an appropriate time we seed the population with a single infected host before each wave i at a fitted time $T_{\text{seed},i}$. We assume that seasonal forcing is sinusoidal and fit both the phase θ_{SF} and amplitude b_{SF} of the modulating function. All models assume that a proportion (of the population) governed by parameter x_I have lasting sterilising protection (compartment P) motivated by observations that antigenic recycling (Ahmed et al., 2007) can give rise to antibody mediated protection in older hosts (Itoh et al., 2009). These hosts may alternatively represent socially isolated groups/individuals.

Our models *must* include the possibility that infection-acquired protection against the pandemic virus is lost in order to explain the reports of repeated symptoms across multiple waves. Acquired immunity wanes at a rate ϕ_w for all candidate models. In model families A–D we trial one model (A1, B1, C1 & D1) in which the rate of loss of acquired protection is constant ($\phi_w \propto 1/T_w$). For all other candidate models (A2, B2, C2 & D2) we assume that acquired immunity is lost at a rate that declines geometrically with each infection n [$\phi_w \propto 1/(T_w \chi_{Tw}^{n-1})$]. The parameter T_w therefore indicates the expected duration of protection following first infection for all model candidates. Boosting of the duration of protection by a factor χ_{Tw} following repeated infections may signal the consolidation of adaptive immune responses against a novel pandemic virus (as sometimes noted following repeated doses of vaccine (Zhu et al., 2009)). Alternatively, increased duration of host protection with each infection may reflect the circulation of a limited number of phenotypically distinct viruses.

Our simplest family of models, A, are captured by the lower *SEIAR* loop in Fig. 1a, and assume that the only form of pre-pandemic immunity is sustained sterilising immunity for a proportion x_I of hosts (compartment P). For models in family B, we allow for the existence of widespread partial sustained prior immunity by stratifying the population into influenza-experienced hosts S_E and influenza-naïve hosts S_N (see Fig. 1a). This pre-pandemic immunity is attributed to hosts beginning in the modified susceptibility state S_E, with abundance determined by the parameter x_E, who experience reduced susceptibility, reduced propensity to report symptoms, and reduced propensity to transmit infection by factors ϵ_S, ϵ_α and ϵ_I, respectively. Such pre-pandemic protection may be afforded by cross-protective cellular and/or humoral immune responses remnant from prior exposure to seasonal IAV variants (e.g. Brown and Kelso, 2009; Krause et al., 2011). In model family B, recovered naïve hosts migrate into the experienced stratum ($R_N \rightarrow S_E$) as the epidemic progresses.

There is no sustained partial prior immunity for models in families C & D. Instead waning sterilising pre-pandemic immunity is attributed to a portion of the population governed by $(1-z)(1-x_I)$ who begin in the compartment Q. In family C this prior immunity is lost at a constant rate ($\phi_{wQ} \propto 1/T_{wQ}$). In family D prior immunity is lost at a variable rate depending on the state of the epidemic ($\phi_{wQ} \propto 1/T_{wQ} + k_{wanQ} I_{\text{cum}}(S+R)/(S+1)$) following the initial seed infection. The latter form, where I_{cum} is the cumulative number of symptomatic and asymptomatic infectious over the epidemic wave and k_{wanQ} is a fitted parameter, may mimic the introduction of a novel IAV variant or viral escape of prior immunity due to the accrual of genetic diversity [$\propto I_{\text{cum}}$] and increase in immunity-driven selective pressure [$\propto (S+R)/(S+1)$] over the course of the first epidemic wave (Boni et al., 2006).

The effective reproduction number R_{eff} depends on the current susceptibility profile of the population and seasonal timing:

$$R_{\text{eff}}(t) = R_0 \frac{S_\star(t)}{N(x_E \epsilon_I \epsilon_S + (1-x_E))} \frac{1}{b_{\text{SF}} \cos(2\pi(t+\theta_{\text{SF}}))}, \quad (1)$$

where N is the population size and t is the time in weeks since the simulation begins (chosen to be 27th May 1918, just over a month prior to the first mortality data point). $S_\star(t) = S_E(t)\epsilon_I\epsilon_S + S_N(t)$ for model families A & B or $S_\star(t) = S(t)$ for model families C & D. Full model details, including differential equations and initial conditions, are provided in the Supplementary Material.

Model fitting and interpretation

We fit each candidate model to the composite data set using Markov Chain Monte Carlo (MCMC) techniques with simulated annealing (Earl and Deem, 2005). We maximise a

pseudo-likelihood calculated by comparing model output to mortality and case reporting data assuming that all counts are Poisson distributed (see Mathews et al., 2007, and Section S2, Supplementary Material). Parameters are assigned either uniform priors or biologically/epidemiologically motivated informative priors, as detailed in full in the Supplementary Material. Briefly, informative priors give preference to values of T_i which result in a serial interval of $\gtrsim$2 days, values of T_w large enough that reinfection within a wave is rare, and large (small) values z (x_I) to preference fits with low to moderately extensive pre-pandemic immunity. We also place priors on $T_{\text{seed},i}$ which peak approximately 2 weeks before the onset of each mortality wave and preference values for the case fatality rate which are in agreement with the survey data and values of θ_{SF} which maximise virus transmissibility in winter. Convergence is assessed by rerunning the MCMC algorithm with randomly assigned initial parameters (Section S3, Supplementary Material).

We estimate the sample size corrected Akaike Information Criteria (AICc) (Akaike, 1974) to compare candidate models. Given uncertainties in viral circulation and adaptive and innate immune responses to the pandemic virus(es), each candidate model is theoretically immunologically defensible. However, parameter estimates across model candidates may show varying biological/epidemiological consistency. Models are ruled implausible if they cannot reproduce most trends in the observed data or if the parameter estimates yield biologically/epidemiologically implausible interpretations. In addition, we assess the ability of plausible candidate models to fit individual city data.

Results

Best fitting model dynamics are shown in Fig. 2 and Supplementary Material Figures S5 & S6. Parameter estimates for all candidate models are shown in Fig. 3 and Supplementary Material Figure S7 and Table S2. Models A1 and B1 – which do not permit boosting of the duration of acquired immunity or waning of prior protection – each predict repeated (unobserved waves of post-pandemic infection (see Figure S5, Supplementary Material). Even if we permit the basic reproduction number to differ between waves in model A1 (denoting this modification model A1*), we cannot reproduce the mortality data well, and the poor fit requires the transmissibility to increase drastically and arguably unrealistically between waves (see Figures S5 & S9, Supplementary Material). We thus exclude models A1 and B1 from further discussion and discuss the interpretation and plausibility of all other candidate models below.

Pre-pandemic protection

The inferred proportion of sterilising pre-pandemic protection for model families C & D [given by $x_E(x_I+(1-z)(1-x_I))$] varies between candidate models. All but D2 of the candidate models in these families prefer $\gtrsim$88% of hosts to have pre-pandemic (permanent or temporary) sterilising protection despite strong priors on z and x_I biasing against such levels. Such widespread sterilising immunity is likely unrealistic given estimates of the fraction of elderly who were protected against new viruses in contemporary pandemics (Itoh et al., 2009), and therefore our fits for models C1, C2 & D1 are arguably also implausible. Temporary pre-pandemic sterilising protection is lost rapidly during the first wave for all but model C1 for these families (for which it is lost more gradually over the three waves).

Having excluded models C1, C2 & D1, only D2 remains a potentially plausible candidate of the models with temporary prior protection. Lower values of pre-pandemic protection of around 40 per cent are inferred for this model, three quarters of which is lost rapidly during the first wave. Such prevalence may be plausible if widespread recent IAV infection offered temporary protection against infection with the newly emerged pandemic virus, or alternatively, exposure to IAVs over previous seasons protected older hosts (Epstein, 2006) but the virus was able to escape this protection during the first wave. Furthermore, with only 1 in 10 exposures being recorded in morbidity data ($\alpha_1 \approx 0.1$), those who did lose their protection rapidly *and* were exposed were highly likely to have a mild (and so unobserved) illness.

Loss of pre-pandemic protection is not *required* to generate a triple-peaked epidemic; one of our simplest models (A2) with only permanent sterilising pre-pandemic protection (due to hosts in P) can roughly fit the case reporting and mortality data (albeit with a poor match to the shape of the first wave, Fig. 2) with around 12 per cent isolated/protected. Including the possibility of partial and sustained pre-pandemic protection (model B2) changes the inferred initial susceptibility profile very little (although acquisition of partial protection – by moving from R_N to S_E in Fig. 1 – following the first infection broadens the first epidemic peak improving the fit to the mortality data).

Transmission parameters

The inferred basic reproduction number varies with candidate model structure. Maximum likelihood values range from ~3.6–10, but are below ~5.5 for all models except C1 & D1 (which we have ruled implausible) and model B2. The posterior distribution of R_0 in model B2 appears bimodal (see Supplementary Material). Whilst the maximum likelihood value is in the higher mode centred around ~10, the lower mode is centred around $R_0 \sim 5$ indicating moderate values of R_0 are not incompatible with this model structure.

The estimated value of R_0 for model D2 is slightly lower than that for our simplest model (A). Whilst for a single epidemic wave estimates of R_0 typically increase with the amount of prior immunity (e.g. Mills et al., 2004), our results highlight that inclusion of pre-pandemic immunity does not necessarily inflate estimates of R_0 for multi-wave pandemics. The model effective reproduction number is very high at the beginning of the simulation for all best-fitting candidates but peaks at 1.2–1.5 for the second and third pandemic waves, consistent with empirical measurements of the growth rate of pH1N11918 in US communities (White and Pagano, 2008).

Despite strong priors biasing the pseudo-likelihood toward infectious periods of 1.6 days, estimates of T_i range from less than half a day to almost 3 days across candidate models. Models C1 & D1 (which have very similar fitted parameter sets) prefer a very low value for T_i consistent with the very high force of infection required to sustain transmission in a population that is slower to lose both prior and acquired protection. Across other candidate models estimates of the serial interval are 3–4.5 days, in keeping with estimates for the Spanish influenza pandemic using mortality data from London (He et al., 2011) and RAF camps (Mathews et al., 2007).

Seasonality of transmission plays a strong role in all plausible model fits, with phase (θ_{SF}) and amplitude (b_{SF}) indicating transmission in the winter months is enhanced by 50–100 per cent compared to summer/autumn. The failure of model B1 to fit a triple peaked epidemic indicates that sinusoidal seasonal forcing alone cannot halt a fourth wave of infection in a simple *SEIAR* transmission model.

Disease severity

Our model fits suggest that asymptomatic infections were common, especially in the first wave, with all plausible models preferring $\alpha_1 \lesssim 0.1$ (i.e. at most 1 in 10 infections was reported

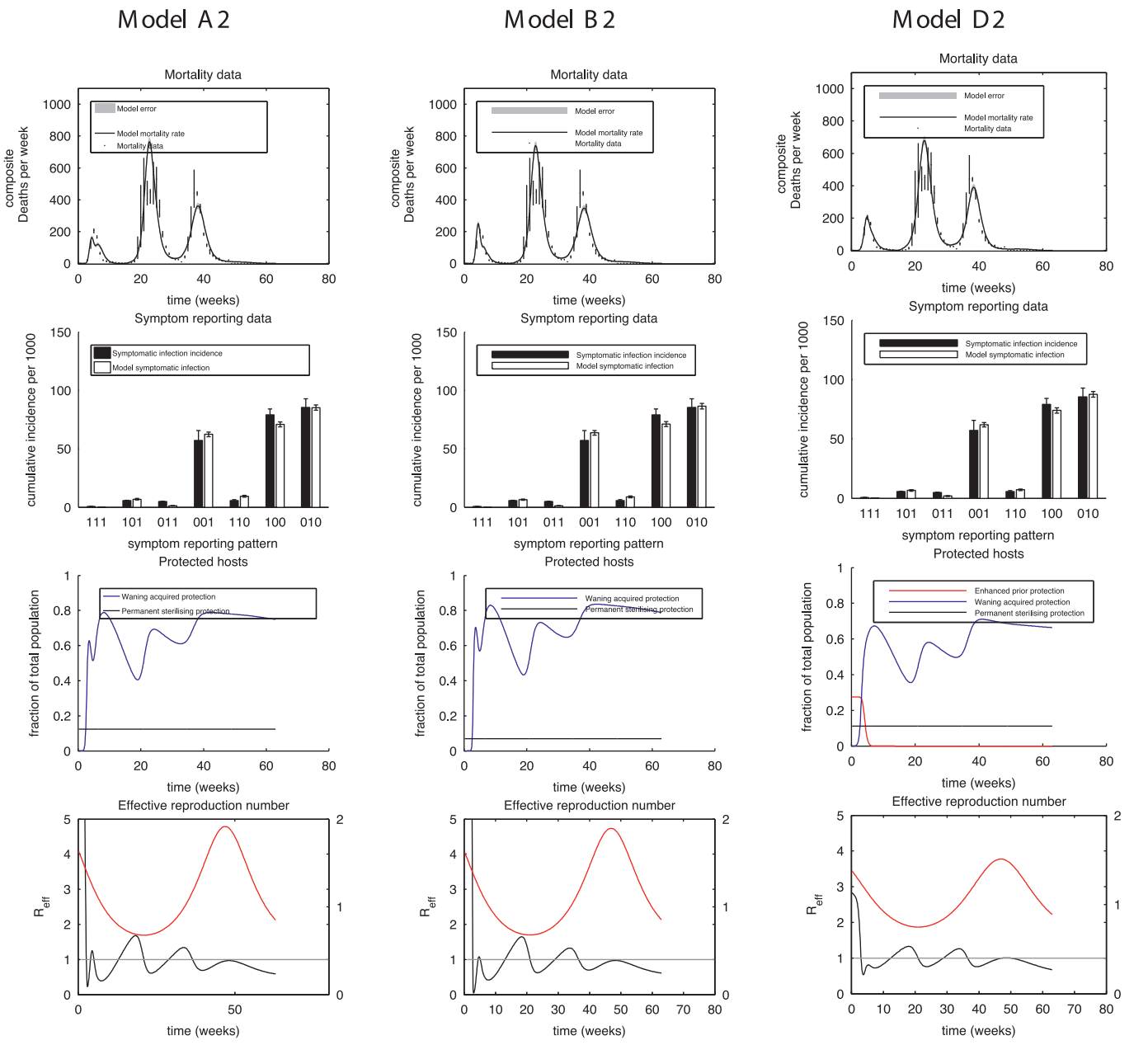

Fig. 2. Model fits to composite data. *Top*: Model fit (solid black line) with Poisson error (grey shaded region) to the weekly mortality data (dots). *Upper middle*: Model fit and Poisson error (white with error bars) for the symptom reporting data with bootstrapped errors (solid black with error bars). The *x*-axis labels *ijk*, with $i, j, k \in \{0, 1\}$ indicate reported illness in waves 1, 2 and/or 3 if i, j and/or $k = 1$, respectively. *Lower middle*: Fraction of population with temporary acquired protection (blue), waning prior protection (red) and permanent sterilising protection (black). *Bottom*: Effective reproduction number as a function of time (black) compared to the threshold value (grey). The seasonal forcing term is plotted in red against the right hand axis. Note that R_{eff} peaks at >5 for models A2 and B2. (For interpretation of the references to colour in this figure legend, the reader is referred to the web version of this article.)

during the herald wave). Higher values for α_i are preferred for later waves indicating relatively more symptomatic infections, but asymptomatic infections (occurring in a proportion $1 - \epsilon_\alpha \alpha_i$) are still far more common than symptomatic infections in waves 2 and 3 for plausible models. Estimated case fatality rates rates (μ_i) are consistent across all models as they are highly constrained by the ratio of reported symptomatic infections and deaths within each wave. Inferred case fatality rates are highest in the second wave (see Figure S7, Supplementary Material). The overall attack rate including asymptomatic (or unreported) infections is in excess of 80 per cent for the models ruled plausible, and highest for models in families A or B. As immunity is on average longer-lasting amongst hosts following the third wave of infection, further epidemics are prevented for 1–2 years for all best fitting models bar A1 and B1.

Acquired protection and virus circulation

Waning of acquired protection is necessary to fit the three waves of mortality and the observations of repeated symptomatic infection amongst some hosts across all model candidates. However only models that include boosting ($\chi_{Tw} > 1$) – ensuring that acquired protection is eventually sustained following repeated infection – yield plausible model fits (models A2, B2, C2). Including boosting also often significantly improves the fit to the symptom reporting data within a given model family (see Table 3). Of the three

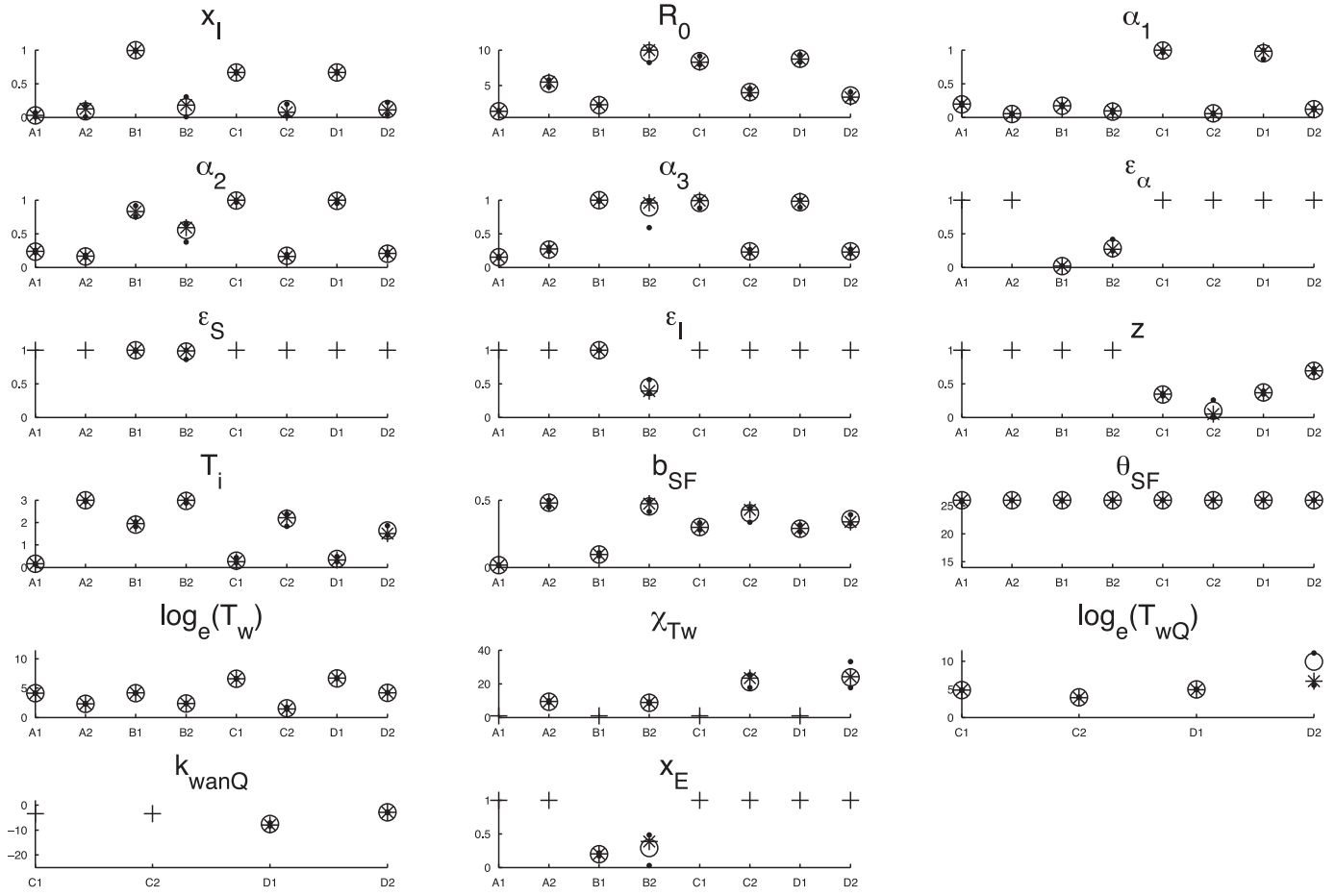

Fig. 3. Maximum likelihood values (stars), 95 per cent credibility regions (straddled by dots) and median values (open circles) for model parameters across candidate models. Crosses indicate the value of fixed parameter values.

plausible models (A2,B2,D2), model D2 is preferred based on AICc alone followed by model B2. The key differences in the interpretation of these models is the acquisition and loss of immunity to the pandemic virus (Table 4).

Estimated boosting factors χ_{Tw} are higher for models in families C & D, and together with longer durations of protection following initial infection T_w, would permit up to 2 infections to occur over the course of the 9 month pandemic. Evidence that children may require two vaccine doses to generate an immunogenic response to a novel virus (Zhu et al., 2009) could support such a boosting model. For the single plausible model within these families (model D2), protection following initial protection is inferred to be ∼3 months. This estimate for T_w is consistent with other analyses of similar data sets suggesting that there is some loss of protection between successive pandemic waves (Mathews et al., 2007; Slepushkin, 1959; Barry et al., 2008).

In contrast, loss of protection following initial infection for models A2 & B2 without prior immunity is particularly short (∼10.5 days), and as many as 3 infections are required for sustained protection. Model based inferences from other influenza epidemics indicate that reinfection over a period of days or weeks can occur (Mathews et al., 2007), consistent with observations that very recent infection does not provide protection against lethal challenge in chickens (Seo and Webster, 2001). However, there is little immunological evidence to suggest that three exposures would be required to generate sustained protection to the same virus, suggesting interpretation of models A2 and B2 requires the circulation of multiple phenotypically distinct lineages. Infections in

Table 3
Comparison of model performance; the number of fitted model parameters (N_{param}), maximum values for the log-pseudo-likelihood (and the break-down into components due to the mortality and symptom reporting data, respectively), sample-size corrected Akaike Information Criteria (AICc), and plausibility of the best fit model for each candidate trialled.

Model	N_{params}	Maximum log-pseudo-likelihood	AICc	Plausibility
A1	15	−2084 (−2032, −52)	4218	× 4th wave
A2	16	−772 (−665, −107)	1587	√
B1	19	−1505 (−1234, −271)	3062	× 4th wave
B2	20	−739 (−638, −101)	1534	√
C1	17	−892 (−598, −294)	1829	×high pre-pandemic immunity (∼88%)
C2	18	−652 (−583, −69)	1354	×high pre-pandemic immunity (∼96%)
D1	18	−837 (−572, −264)	1724	×high pre-pandemic immunity (∼88%)
D2	19	−630 (−532, −98)	1313	√

Table 4
Model parameter descriptions. Full definitions are given in Table S1, Supplementary Material.

Parameter	Description
R_0	Basic reproduction number
α_i	(Unscaled) symptomatic proportion in ith wave
x_E	Fraction with partial sustained prior immunity
x_I	Fraction with lasting prior sterilising protection
z	Fraction of population beginning in S rather than Q
T_i	Infectious period in days
T_e	Latent period following exposure
b_{SF}	Amplitude of seasonal forcing term
θ_{SF}	Phase of seasonal forcing term
$T_{seed,i}$	Seeding time for ith wave in days after 27th May 1918
T_w	Timescale of acquired sterilising protection
T_{wQ}	Timescale of prior sterilising protection
μ_i	Case fatality rate in the ith wave
ϵ_α	Scale factor for symptomatic proportion in experienced strata
ϵ_S	Scale factor for susceptibility in experienced strata
ϵ_I	Scale factor for infectiousness in experienced strata
k_{wanQ}	Scaling for acceleration of loss of prior protection

model B2 still induce lasting protection against disease; parameter estimates are consistent with a reduction in the probability of symptomatic infection upon reinfection of 70% ($\epsilon_\alpha \sim 0.3$). The maximum-likelihood fit for model B2 also prefers $\epsilon_I < 1$, indicating a reduction in viral shedding for those in the experienced class (see Fig. 1). However the infectiousness of experienced hosts is indistinguishable from that of naïve hosts ($\epsilon_I \sim 1$) for values of R_0 in the lower mode for this model. Estimating population-level transmissibility from epidemiological data for such a model will be aided by results of controlled experiments to isolate the determinants of virus transmissibility.

Fits to individual city data

All three models ruled plausible based on their ability to fit the composite data set (A2, B2, D2) yield reasonable fits to the mortality and symptom reporting data for the original locations (see Figures S17–S22, Supplementary Material). Maximum-likelihood parameters are similar between cities for many, but not all, parameters (see Section S3 and Figures S23–25, Supplementary Material). Given that stochastic effects (He et al., 2011) and demographic differences may generate regional variation in observed epidemiology, some variation is not surprising and reinforces the value of fitting to an aggregated data set in which demographic and stochastic variability is suppressed. Fitting a hierarchical model that constrains the distribution of parameter estimates between locations may improve the consistency of parameter estimates for individual city fits (Mathews et al., 2010), however as our fit to the composite data set already provides a (less computationally intensive) route to extracting parameter estimates representative of the total data set, and we do not explore this option further here.

Conclusions

We have introduced a novel family of immunologically motivated models of influenza transmission to describe the patterns of mortality, infection and re-infection as observed in the 1918–19 UK influenza pandemic. Where others have previously examined only mortality data, our multi-dimensional analysis provides new insights into the likely role of pre-existing and temporary immunity. Our results suggest that heterosubtypic and cross-protective immune responses are an important factor in understanding the multi-wave behaviour of influenza pandemics.

Previous analyses of 1918–19 case reporting data in the UK have suggested that illness in one wave conferred some protection in subsequent waves (Barry et al., 2008; Mathews et al., 2010), and yet illness in multiple waves in an individual was noted in each of the five cities under study. We have shown that three of our eight candidate biologically motivated dynamical models, each assuming different roles for pre-pandemic and acquired immunity to the novel virus, can capture most of the observed features of the symptom reporting and mortality data in the subset of English cities for which the necessary data is available. Estimates for R_0 vary from 3.5 to 10 across our plausible model candidates, but are more moderate ∼5–6 when hosts with pre-pandemic influenza experience are assumed to be fully infectious (i.e. models A2 and D2). Assuming only seasonal changes in the basic reproduction number R_0, we infer seasonal forcing to be strong (amplitude b_{SF}) with transmission peaking during winter (θ_{SF}) for all plausible candidate models. However seasonal forcing alone cannot halt "out of season" activity following the third/winter wave without imposing additional constraints on the number of infections per host (through the boosting factor χ_{Tw}). In all models, loss of infection-acquired immunity (on a time-scale T_w) is key to explaining multiple waves of infection in the absence of strong heterogeneous or complex time-dependent mixing effects. Together with low values for the proportion of infections that are symptomatic (α_i) our plausible model candidates can approximately reproduce the fraction of hosts experiencing symptomatic infections in multiple waves reported in the survey symptom reporting data.

A model similar to that used to model the double peaked epidemic observed in RAF camps (Mathews et al., 2007) and attack rates in English cities and schools (Mathews et al., 2010) is our preferred candidate model (D2) based on its Akaike information criterion when fitting to the composite data set. In this model we find that a variable rate of loss of prior immunity that allows for delayed and rapid loss of population-level prior immunity (from state Q), rather than constant rate of loss used in our previous models, is required to recover epidemiologically plausible estimates for the extent of pre-pandemic sterilising immunity when fitting to the composite data set. While this candidate model can also fit the data set for each individual location comprising the composite data set, an exponential rate of loss of prior immunity with similar timing is preferred for all individual locations, indicating that our modelling has limited power to discriminate between mechanisms for the loss of the prior immunity. Nevertheless, across all individual data sets *and* our composite sets, a single change in viral phenotype triggering loss of prior protection during the first wave, combined with the low probability of reporting symptoms and heterologous cross-protection following initial infection with a pandemic variant that lasts ∼3 months, can explain the pattern of reported morbidity and mortality in 1918–19.

Loss of pre-pandemic protection is not required to fit the triple peaked epidemic data, as is evident in the fits of models A2 and B2. However, without replenishment of the susceptible pool from a previously immune pool (Q), rapid loss of acquired protection (T_w) during the first wave is required to fuel the repeated waves of infection (models A2, B2). Such a pattern of susceptibility could indicate the circulation of up to 3 phenotypically distinct influenza viruses over the course of the three waves. Alternatively, the very rapid loss of immunity following initial infection could signal that our simple model for infection-acquired immunity is inappropriate for capturing the development and maintenance of adaptive immunity over the pandemic period.

Assessing the relative plausibility of our model inferences regarding adaptive immunity to pandemic IAV in plausible candidates is difficult, particularly given the lack of data on the characteristics of the circulating viruses. Neutralising antibody titres following confirmed infection with pH1N12009 were deemed protective in only around 90 per cent of hosts (Hung et al., 2010), suggesting a deficient immune response may enable reinfection with the same virus in some people. Symptomatic reinfection with

pH1N12009 was noted amongst a handful of cases (Perez et al., 2010; Trakulsrichai et al., 2012), over a range of time-periods from 2 weeks to 5 months. Modelling studies (Mathews et al., 2007; Camacho et al., 2011) and animal challenge studies (Seo and Webster, 2001) also suggest that delays in the development of adaptive immunity may admit a window of opportunity for symptomatic reinfection following recovery. The mechanisms governing the possibility of symptomatic reinfection of hosts in pandemic scenarios are complex (see Trakulsrichai et al., 2012) and to probe these more deeply would likely require further data on repeated challenge in human subjects.

Comparison to previous work

Maximum likelihood estimates for R_0 vary across plausible model candidates but are consistent with those inferred using similar models for immunity in our previous work (Mathews et al., 2007, 2010). Noting that as we fit to both mortality and symptom reporting data rather than mortality data alone, and are therefore able to consider the impact of asymptomatic infection, all of our estimates for R_0 are significantly higher than those inferred by He et al. (2011, 2013). Without the constraint of matching re-infection data in their analyses, He et al. were able to model dynamics with a median $R_0 = 2.36$ and variations in transmissibility that are purely driven by changes in population mixing rates and climatic effects. Models for pH1N11918 transmission which assume the circulation of multiple phenotypes with different values of R_0 (Rios-Doria and Chowell, 2009), similar to our model A1*, would likely fit the data utilised here by allowing for wave-dependent transmissibility. Variation in estimates of transmissibility depending on underlying model assumptions reinforce the importance of understanding the climatic, sociological and virological determinants of transmission in order to estimate the true fitness of pandemic viruses and the causes of multi-wave epidemic behaviour.

We infer a very strong role for seasonal forcing in which transmission in the winter is enhanced by 50–100 per cent. Such an effect is unlikely purely due to climatic factors (Shaman et al., 2009). Decreased transmission during the summer months may also be due to changes in mixing triggered by school holidays (Eames et al., 2012). Indeed He et al. report a significant forcing effect due to school term times of around 30 per cent (He et al., 2013).

Our preferred model, with fixed intrinsic viral transmissibility but heterogeneity in prior protection and the longevity of acquired protection, is consistent with independent analyses of this pandemic. Fits to our preferred model D2 suggest prior immunity in influenza-experienced hosts protects this cohort at the beginning of the first wave, and thus is qualitatively consistent with independent analyses indicating negative correlations between population age and herald wave severity (Pearce et al., 2011). Regardless of the mechanisms driving changes in host immunity, our inference of significant loss of both recently acquired and prior protection before the end of the first wave is congruent with the widely discussed hypothesis that the summer wave of the 1918 pandemic in Europe was caused by a highly transmissible virus with relatively moderate pathogenesis that partially immunised the population against a more pathogenic virus that was responsible for the autumn and winter waves (Barry et al., 2008; Mathews et al., 2010; Olson et al., 2005), even though this was not an *a priori* assumption. Estimates of higher symptom reporting and death rates for the second and third waves are also consistent with such a hypothesis. Because exposure during the first wave was unlikely to result in clinical presentation ($\alpha_1 \approx 0.1$), this explanation (model D2) is not at odds with the lack of direct epidemiological evidence for a significant loss of immunity during the first wave(s) of the pandemic and indeed may be considered as a prompt for further investigation.

Study limitations

Our model attributes heterogeneities in population susceptibility to immunological rather than sociological, demographic or (non-seasonal) environmental effects, and thus may overestimate the role of population immunity in moderating epidemic dynamics. A population influx, for example due to the return of troops following the end of First World War combat, could also have provided "the fuel" for a severe second wave. Virus circulation had already reached pandemic proportions prior to the autumn and outbreaks in military camps were noted over the summer (see Smallman-Raynor et al., 2002, and references therein). It therefore seems unlikely that troop movement significantly increased the proportion of the population who were susceptible, although mixing patterns and/or intensity may have been altered. The seasonal modulation of transmission included in our model limits transmission during the summer months and thus may mimic the influence of reduced mixing during summer holidays. Suppressed mixing during winter due to school holidays may also be a driver of multi-wave influenza pandemic transmission (Kubiak and McLean, 2012). More complex temporal changes in transmissibility due to temperature and humidity are possibly also relevant for understanding pandemic dynamics (Shaman et al., 2011). Reactive social distancing may also have been important in this setting (He et al., 2013).

It is also possible that our model does not have the appropriate structure to capture the dynamics of within host adaptive immunity. Temporary partial immunity following recovery may better describe the immune response to new viruses (Ferguson et al., 2003). Allowing for a delay in the development of adaptive immunity may be relevant in some contexts (Camacho et al., 2011) and suboptimal immune responses due to original-antigenic-sin like phenomena (Monsalvo et al., 2011) may be required to capture changing host immunity (even to the same virus) over short time-scales. Mechanisms other than escape of prior immunity such as immune-complex mediated disease (Monsalvo et al., 2011), cytokine storm effects (de Jong et al., 2006) and/or an evolution in virulence (Taubenberger and Kash, 2011) may also be responsible for increased disease severity in later waves.

Age-dependent attack rates and mortality were observed in sub-populations in 1918–19 (Shanks and Brundage, 2012). Changes in the age-distribution of cases with time was also noted in the 2009 pandemic (Pebody et al., 2010). Although age was likely an important determinant of susceptibility, mixing characteristics, propensity to report symptoms and likelihood of death, we do not have the age-dependent mortality or morbidity data to constrain an age-dependent transmission model.

The case reporting data we have used is essential for constraining case fatality rates and the time-scale for loss of immunity, however it is difficult to assign uncertainty to the available estimates of the symptomatic attack rates given that they are based on patient reporting data that were often collected by untrained staff (Ministry of Health, 1920, p. 453) over an extended period following the epidemic. There are additional concerns about the consistency of the data collected in Manchester (Ministry of Health, 1920, p. 488). Circulation of other respiratory viruses such as Influenza B and RSV may also spuriously increase the reported proportion of hosts experiencing repeated symptomatic infections. We have only briefly considered the significance of differences in mortality and symptom reporting rates between cities studied. In future work we will consider whether demographic differences in prior immunity and climatic variation between the cities under study can explain regional variations in the pattern of mortality and morbidity.

Implications

The data available to constrain epidemiological models for the 1918–19 pandemic are limited, and as a result some parameters in our candidate models (particularly model B2) are difficult to identify. Many data sources typically available for contemporary pandemics would improve parameter identifiability and enable richer tests of models for heterologous immunity in transmission dynamics. Longitudinal serological data would provide stronger constraints on pre-pandemic immunity and the proportion of symptomatic infections (Hoschler et al., 2012). Temporal phylogenetic characterisation of circulating viruses would enable well motivated constraints on the timing of emergence of new variants (Yang et al., 2011) and surveys of mixing patterns (Eames et al., 2012) would enable the influence of school term times or reactive social distancing to be incorporated as additional seasonal factors in transmission (*sensu* He et al., 2013).

Our modelling indicates that viral escape of prior immunity is consistent with pandemic influenza dynamics in 1918–19, and may explain the observations of more severe disease in the second wave of infection. While we cannot infer the genesis of prior immunity in our model, widespread prior immunity due to recognition of T cell epitopes would be broadly consistent with evidence that many adults exhibited CD8+ T cell responses to pH1N12009 (Groot et al., 2009; Scheible et al., 2011). Antibodies to conserved regions of the haemaglutinin stalk may also mediate partial heterosubtypic immunity relevant for a pandemic virus (Ellebedy and Ahmed, 2012). Despite significant evidence that heterologous immune response may dampen the impact of a pandemic, a pandemic virus with novel antigenic type that has not circulated in humans in the last century like H7N9 (Liu et al., 2013) would likely have devastating impact if it possessed transmissibility similar to that of pH1N11918.

Immunological determinants of prior immunity to novel or emerging pandemic viruses beyond the existence of protective antibody are still incompletely understood, but may prove crucial for predicting and controlling the severity of pandemic influenza. Viral surveillance data which includes characterisation of T-cell epitopes, antigenic glycosylation and haemaglutinin stalk architecture would help constrain models for the influence of heterosubtypic immunity on influenza epidemiology. Models that can capture the population-level consequence of changes in heterologous protection would be better placed to anticipate pandemic influenza severity and consider the appropriate use of novel vaccines which aim to induce heterologous cross protection.

Acknowledgments

We thank the NHMRC for supporting this work through grants 400588, 454645, 566908 and 628977. KB acknowledges support from a University of Melbourne McKenzie Postdoctoral Fellowship and visitor support from the University of Nottingham. JMcCaw acknowledges support from an ARC Future Fellowship and JMcVernon the NHMRC. Funds from a University of Melbourne Interdisciplinary Seed Grant were used to consult with the Victorian Partnership of Advanced Computing to develop optimal techniques for simulating the model system. The authors would like to acknowledge exploratory work undertaken by P. Pallaghy, provision of data by D. Pearce and useful discussions with E. McBryde.

Appendix A. Supplementary data

Supplementary data associated with this article can be found, in the online version, at http://dx.doi.org/10.1016/j.epidem.2014.07.004.

References

Ahmed, R., Oldstone, M.B.A., Palese, P., 2007. Protective immunity and susceptibility to infectious diseases: lessons from the 1918 influenza pandemic. Nat. Immunol. 8, 1188–1193.

Akaike, H., 1974. A new look at the statistical model identification. IEEE Trans. Autom. Control 19, 716–723.

Barry, J.M., Viboud, C., Simonsen, L., 2008. Cross-protection between successive waves of the 1918–1919 influenza pandemic: epidemiological evidence from us army camps and from Britain. J. Infect. Dis. 198, 1427–1434.

Boni, M., Gog, J., Andreasen, V., Feldman, M., 2006. Epidemic dynamics and antigenic evolution in a single season of influenza A. Proc. Biol. Sci. 273, 1307–1316.

Bootsma, M., Ferguson, N., 2007. The effect of public health measures on the 1918 influenza pandemic in U.S. cities. Proc. Natl. Acad. Sci. U.S.A. 104, 7588–7593.

Brown, L.E., Kelso, A., 2009. Prospects for an influenza vaccine that induces cross-protective cytotoxic T lymphocytes. Immunol. Cell Biol. 87, 300–308.

Caley, P., Philp, D.J., McCracken, K., 2008. Quantifying social distancing arising from pandemic influenza. J. R. Soc. Interface 5, 631–639.

Camacho, A., Ballesteros, S., Graham, A.L., Carrat, F., Ratmann, O., Cazelles, B., 2011. Explaining rapid reinfections in multiple-wave influenza outbreaks: Tristan da Cunha 1971 epidemic as a case study. Proc. Biol. Sci. 278, 3635–3643.

Chowell, G., Bettencourt, L., Johnson, N., Alonso, W., Viboud, C., 2008. The 1918–1919 influenza pandemic in England and Wales: spatial patterns in transmissibility and mortality impact. Proc. Biol. Sci. 275, 501–509.

dos Reis, M., Tamuri, A.U., Hay, A.J., Goldstein, R.A., 2011. Charting the host adaptation of influenza viruses. Mol. Biol. Evol. 28, 1755–1767.

Eames, K.T.D., Tilston, N.L., Brooks-Pollock, E., Edmunds, W.J., 2012. Measured dynamic social contact patterns explain the spread of H1N1v influenza. PLoS Comput. Biol. 8, e1002425.

Earl, D.J., Deem, M.W., 2005. Parallel tempering: theory, applications, and new perspectives. Phys. Chem. Chem. Phys. 7, 3910–3916.

Efron, B., 1979. Bootstrap methods: another look at the Jacknife. Ann. Stat. 7, 1–26.

Eggo, R.M., Cauchemez, S., Ferguson, N.M., 2010. Spatial dynamics of the 1918 influenza pandemic in England, Wales and the United States. J. R. Soc. Interface 8, 233–243.

Ellebedy, A.H., Ahmed, R., 2012. Re-engaging cross-reactive memory b cells: the influenza puzzle. Front. Immunol. 3, 53.

Epstein, S., 2006. Prior H1N1 influenza infection and susceptibility of Cleveland family study participants during the H2N2 pandemic of 1957: an experiment of nature. J. Infect. Dis. 193, 49–53, 0022-1899.

Ferguson, N., Galvani, A., Bush, R., 2003. Ecological and immunological determinants of influenza evolution. Nature 422, 428–433.

Fraser, C., Cummings, D.A.T., Klinkenberg, D., Burke, D.S., Ferguson, N.M., 2011. Influenza transmission in households during the 1918 pandemic. Am. J. Epidemiol. 174, 505–514.

Grebe, K.M., Yewdell, J.W., Bennink, J.R., 2008. Heterosubtypic immunity to influenza a virus: where do we stand? Microbes Infect. 10, 1024–1029.

Groot, A.S.D., Ardito, M., McClaine, E.M., Moise, L., Martin, W.D., 2009. Immunoinformatic comparison of T-cell epitopes contained in novel swine-origin influenza A (H1N1) virus with epitopes in 2008–2009 conventional influenza vaccine. Vaccine 27, 5740–5747.

He, D., Dushoff, J., Day, T., Ma, J., Earn, D., 2011. Mechanistic modelling of the three waves of the 1918 influenza pandemic. Theor. Ecol. 4, 283–288, http://dx.doi.org/10.1007/s12080-011-0123-3.

He, D., Dushoff, J., Day, T., Ma, J., Earn, D.J.D., 2013. Inferring the causes of the three waves of the 1918 influenza pandemic in England and Wales. Proc. R. Soc. Lond. B: Biol. Sci. 280, 20131345 http://rspb.royalsocietypublishing.org/content/280/1766/20131345.full.pdf+html

Hoschler, K., Thompson, C., Andrews, N., Galiano, M., Pebody, R., Ellis, J., Stanford, E., Baguelin, M., Miller, E., Zambon, M., 2012. Seroprevalence of influenza A(H1N1)pdm09 virus antibody, England, 2010 and 2011. Emerg. Infect. Dis. 18, 1894–1897.

Hung, I.F.N., To, K.K.W., Lee, C.K., Lin, C.K., Chan, J.F.W., Tse, H., Cheng, V.C.C., Chen, H., Ho, P.L., Tse, C.W.S., Ng, T.K., Que, T.L., Chan, K.H., Yuen, K.Y., 2010. Effect of clinical and virological parameters on the level of neutralizing antibody against pandemic influenza A virus H1N1 2009. Clin. Infect. Dis. 51, 274–279.

Itoh, Y., Shinya, K., Kiso, M., Watanabe, T., Sakoda, Y., Hatta, M., Muramoto, Y., Tamura, D., Sakai-Tagawa, Y., Noda, T., Sakabe, S., Imai, M., Hatta, Y., Watanabe, S., Li, C., Yamada, S., Fujii, K., Murakami, S., Imai, H., Kakugawa, S., Ito, M., Takano, R., Iwatsuki-Horimoto, K., Shimojima, M., Horimoto, T., Goto, H., Takahashi, K., Makino, A., Ishigaki, H., Nakayama, M., Okamatsu, M., Takahashi, K.W., 2009. In vitro and in vivo characterization of new swine-origin H1N1 influenza viruses. Nature 460, 1021–1025.

de Jong, M.D., Simmons, C.P., Thanh, T.T., Hien, V.M., Smith, G.J.D., Chau, T.N.B., Hoang, D.M., Chau, N.V.V., Khanh, T.H., Dong, V.C., Qui, P.T., Cam, B.V., Ha, D.Q., Guan, Y., Peiris, J.S.M., Chinh, N.T., Hien, T.T., Farrar, J., 2006. Fatal outcome of human influenza a (H5N1) is associated with high viral load and hypercytokinemia. Nat. Med. 12, 1203–1207.

Krause, J.C., Tsibane, T., Tumpey, T.M., Huffman, C.J., Basler, C.F., Crowe, J.E., 2011. A broadly neutralizing human monoclonal antibody that recognizes a conserved, novel epitope on the globular head of the influenza H1N1 virus hemagglutinin. J. Virol. 85, 10905–10908.

Kubiak, R.J., McLean, A.R., 2012. Why was the 2009 influenza pandemic in England so small? PLoS ONE 7, e30223.

Liu, D., Shi, W., Shi, Y., Wang, D., Xiao, H., Li, W., Bi, Y., Wu, Y., Li, X., Yan, J., Liu, W., Zhao, G., Yang, W., Wang, Y., Ma, J., Shu, Y., Lei, F., Gao, G.F., 2013. Origin

and diversity of novel avian influenza A H7N9 viruses causing human infection: phylogenetic, structural, and coalescent analyses. Lancet 381, 1926–1932.
Mathews, J.D., McBryde, E.S., McVernon, J., Pallaghy, P.K., McCaw, J.M., 2010. Prior immunity helps to explain wave-like behaviour of pandemic influenza in 1918–9. BMC Infect. Dis. 10, 128.
Mathews, J.D., McCaw, C.T., McVernon, J., McBryde, E.S., McCaw, J.M., 2007. A biological model for influenza transmission: pandemic planning implications of asymptomatic infection and immunity. PLoS ONE 2, e1220.
McMichael, A., Gotch, F., Noble, G., Beare, P., 1983. Cytotoxic T-cell immunity to influenza. N. Engl. J. Med. 309, 13–17.
Mills, C., Robins, J., Lipsitch, M., 2004. Transmissibility of 1918 pandemic influenza. Nature 432, 904–906, 1476-4687.
Ministry of Health, 1920. Pandemic of Influenza 1918–9. Number 4 in Reports on Public Health and Medical Subjects. His Majesty's Stationery Office, London, United Kingdom, Available from FluWeb Historical Influenza Database, http://influenza.sph.unimelb.edu.au (accessed September 2012).
Monsalvo, A.C., Batalle, J.P., Lopez, M.F., Krause, J.C., Klemenc, J., Hernandez, J.Z., Maskin, B., Bugna, J., Rubinstein, C., Aguilar, L., Dalurzo, L., Libster, R., Savy, V., Baumeister, E., Aguilar, L., Cabral, G., Font, J., Solari, L., Weller, K.P., Johnson, J., Echavarria, M., Edwards, K.M., Chappell, J.D., Crowe, J.E., Williams, J.V., Melendi, G.A., Polack, F.P., 2011. Severe pandemic 2009 H1N1 influenza disease due to pathogenic immune complexes. Nat. Med. 17, 195–199.
Morens, D.M., Fauci, A.S., 2007. The 1918 influenza pandemic: insights for the 21st century. J. Infect. Dis. 195, 1018–1028.
Murray, C., Lopez, A., Chin, B., Feehan, D., Hill, K., 2006. Estimation of potential global pandemic influenza mortality on the basis of vital registry data from the 1918–20 pandemic: a quantitative analysis. Lancet 368, 2211–2218.
Nguyen-Van-Tam, J.S., Hampson, A.W., 2003. The epidemiology and clinical impact of pandemic influenza. Vaccine 21, 1762–1768.
Olson, D., Simonsen, L., Edelson, P., Morse, S., 2005. Epidemiological evidence of an early wave of the 1918 influenza pandemic in New York City. Proc. Natl. Acad. Sci. U.S.A. 102, 11059–11063.
Pearce, D.C., Pallaghy, P.K., McCaw, J.M., McVernon, J., Mathews, J.D., 2011. Understanding mortality in the 1918-1919 influenza pandemic in England and Wales. Influenza Other Respir. Viruses 5, 89–98.
Pebody, R.G., McLean, E., Zhao, H., Cleary, P., Bracebridge, S., Foster, K., Charlett, A., Hardelid, P., Waight, P., Ellis, J., Bermingham, A., Zambon, M., Evans, B., Salmon, R., McMenamin, J., Smyth, B., Catchpole, M., Watson, J., 2010. Pandemic influenza A (H1N1) 2009 and mortality in the United Kingdom: risk factors for death, April 2009 to March 2010. Euro Surveill. 15.
Perez, C.M., Ferres, M., Labarca, J.A., 2010. Pandemic (H1N1) 2009 reinfection, chile. Emerg. Infect. Dis. 16, 156–157.
Reid, A., Fanning, T., Janczewski, T., Lourens, R., Taubenberger, J., 2004. Novel origin of the 1918 pandemic influenza virus nucleoprotein gene. J. Virol. 78, 12462–12470.
Reid, A.H., Janczewski, T.A., Lourens, R.M., Elliot, A.J., Daniels, R.S., Berry, C.L., Oxford, J.S., Taubenberger, J.K., 2003. 1918 influenza pandemic caused by highly conserved viruses with two receptor-binding variants. Emerg. Infect. Dis. 9, 1249–1253.
Rios-Doria, D., Chowell, G., 2009. Qualitative analysis of the level of cross-protection between epidemic waves of the 1918–1919 influenza pandemic. J. Theor. Biol. 261, 584–592.
Scheible, K., Zhang, G., Baer, J., Azadniv, M., Lambert, K., Pryhuber, G., Treanor, J.J., Topham, D.J., 2011. CD8+ T cell immunity to 2009 pandemic and seasonal H1N1 influenza viruses. Vaccine 29, 2159–2168.
Seo, S.H., Webster, R.G., 2001. Cross-reactive, cell-mediated immunity and protection of chickens from lethal H5N1 influenza virus infection in Hong Kong poultry markets. J. Virol. 75, 2516–2525.
Shaman, J., Goldstein, E., Lipsitch, M., 2011. Absolute humidity and pandemic versus epidemic influenza. Am. J. Epidemiol. 173, 127–135.
Shaman, J., Pitzer, V., Viboud, C., Lipsitch, M., Grenfell, B., 2009. Absolute humidity and the seasonal onset of influenza in the continental US. PLoS Curr. 1, RRN1138.
Shanks, G.D., Brundage, J.F., 2012. Pathogenic responses among young adults during the 1918 influenza pandemic. Emerg. Infect. Dis. 18, 201–207.
Shi, P., Keskinocak, P., Swann, J.L., Lee, B.Y., 2010. Modelling seasonality and viral mutation to predict the course of an influenza pandemic. Epidemiol. Infect., 1–10.
Slepushkin, A.N., 1959. The effect of a previous attack of A1 influenza on susceptibility to A2 virus during the 1957 outbreak. Bull. World Health Organ. 20, 297–301.
Smallman-Raynor, M., Johnson, N., Cliff, A.D., 2002. The spatial anatomy of an epidemic: influenza in London and the county boroughs of England and Wales, 1918–19. Trans. Inst. Br. Geogr. 27, 452–470.
Smith, G.J.D., Bahl, J., Vijaykrishna, D., Zhang, J., Poon, L.L.M., Chen, H., Webster, R.G., Peiris, J.S.M., Guan, Y., 2009. Dating the emergence of pandemic influenza viruses. Proc. Natl. Acad. Sci. U.S.A. 106, 11709–11712.
Taubenberger, J., Morens, D., 2006. 1918 influenza: the mother of all pandemics. Emerg. Infect. Dis. 12, 15–22.
Taubenberger, J.K., Kash, J.C., 2011. Insights on influenza pathogenesis from the grave. Virus Res. 162, 2–7.
Trakulsrichai, S., Watcharananan, S.P., Chantratita, W., 2012. Influenza A (H1N1) 2009 reinfection in Thailand. J. Infect. Public Health 5, 211–214.
Valleron, A.J., Cori, A., Valtat, S., Meurisse, S., Carrat, F., Bolle, P.Y., 2010. Transmissibility and geographic spread of the 1889 influenza pandemic. Proc. Natl. Acad. Sci. U.S.A. 107, 8778–8781.
Viboud, C., Grais, R.F., Lafont, B.A.P., Miller, M.A., Simonsen, L., Group, M.I.S.M.S., 2005. Multinational impact of the 1968 Hong Kong influenza pandemic: evidence for a smoldering pandemic. J. Infect. Dis. 192, 233–248.
White, L.F., Pagano, M., 2008. Transmissibility of the influenza virus in the 1918 pandemic. PLoS ONE 3, e1498.
Wilkinson, T.M., Li, C.K.F., Chui, C.S.C., Huang, A.K.Y., Perkins, M., Liebner, J.C., Lambkin-Williams, R., Gilbert, A., Oxford, J., Nicholas, B., Staples, K.J., Dong, T., Douek, D.C., McMichael, A.J., Xu, X.N., 2012. Preexisting influenza-specific CD4+ T cells correlate with disease protection against influenza challenge in humans. Nat. Med. 18, 274–280.
Yang, J.R., Huang, Y.P., Chang, F.Y., Hsu, L.C., Lin, Y.C., Su, C.H., Chen, P.J., Wu, H.S., Liu, M.T., 2011. New variants and age shift to high fatality groups contribute to severe successive waves in the 2009 influenza pandemic in Taiwan. PLoS ONE 6, e28288.
Zhu, F.C., Wang, H., Fang, H.H., Yang, J.G., Lin, X.J., Liang, X.F., Zhang, X.F., Pan, H.X., Meng, F.Y., Hu, Y.M., Liu, W.D., Li, C.G., Li, W., Zhang, X., Hu, J.M., Peng, W.B., Yang, B.P., Xi, P., Wang, H.Q., Zheng, J.S., 2009. A novel influenza A (H1N1) vaccine in various age groups. N. Engl. J. Med. 361, 2414–2423.